Loads in the design of flight vehicles

Dorin LOZICI-BRÎNZEI*, Radu BÎSCĂ*, Simion TĂTARU**

*Corresponding author
*INCAS - National Institute for Aerospace Research "Elie Carafoli"
Bdul Iuliu Maniu 220, Bucharest 061136, Romania
lozicid@incas.ro
**Aerospace Consulting Bucharest
Bdul Iuliu Maniu 220, Bucharest 061136, Romania
aerocon@incas.ro
DOI: 10.13111/2066-8201.2010.2.3.6

Abstract: *The calculation of flight loads is a critical part of air vehicle design. On the other hand, the prediction of accurate loads is a sophisticated and complex process that requires skilled and experienced engineers. They must integrate results from wind tunnel tests, computer simulations, historical data and empirical formulations into a number of loads cases that provide a realistic assessment of the flight vehicle's environment. Under these conditions, the vehicle must satisfy requirements imposed by regulatory agencies as part of the vehicle certification process.*
Loads and boundary conditions can be associated to either the finite element model or the underlying geometry. By associating loads and boundary conditions to the geometry the finite element model mesh and elements can be modified without redefining and applying the loads to the model. Loads and boundary conditions are associated to the model geometry by default.

Key Words: flight loads, boundary conditions, assessment of the flight vehicle's environment, finite element method.

1. INTRODUCTION

With FEM analysis, static loads are applied to geometric and scalar points in a variety of ways, including:

- Loads directly applied directly to grid points.
- Pressure loads on surfaces.
- Distributed and concentrated loads on elements.
- Gravity loads.
- Centrifugal loads due to steady rotation.
- Tangential loads due to angular acceleration.
- Loads resulting from thermal expansion.
- Loads resulting from enforced deformations of a structural element.
- Loads resulting from enforced displacements at a grid point.

The import capability allows the user to retrieve an aerodynamic model into the current FEM analysis database.

2. AERO-STRUCTURE COUPLING

The aerodynamic and structural models are created and exist as completely separate entities. In the FEM database, any number of structural models and aerodynamics models may exist. To perform an analysis, a pair of these models must be connected to each other.

In aeroelasticity, generating the model so that the aerodynamic forces can be mapped to the structural model (with equilibrium preservation) and than the structural deformation be mapped to the aerodynamic model allowing aeroelastic forces to be computed, is essential. It is the aero-structure coupling that brings these two models together using splining concepts.

There are two basic methods for splines: beam splines and surface splines. In general, beam splines work well for high aspect ratio wings, bodies and for beam structural models. Surface splines are suitable for low aspect ratio wings and all built-up structures. Note that, in general, it is the nature of the structural model that determines the best spline choice

3. LOAD SUMMATION – METHODOLOGY

For forces, the load summation calculation is simply the summation of the force vector components (transformed if necessary). The moments are calculated by determining the cross product of the force vector and the moment arm vector where the last is a vector from the reference point to the node on which the force vector is applied,

$$\begin{bmatrix} M_x \\ M_y \\ M_z \end{bmatrix} = \begin{bmatrix} F_x F_y F_z \end{bmatrix} \times \begin{bmatrix} d_x \\ d_y \\ d_z \end{bmatrix} \tag{1}$$

For pressure loads, the equivalent nodal loads must be calculated. The first step is to transform the element face to a local coordinate system whose normal, the vector , is defined by the cross product of a vector from node1 to node 2, the vector , of the face and a vector from node 1 to node 4,

$$\begin{bmatrix} u_x \\ u_y \\ u_z \end{bmatrix} = \begin{bmatrix} \gamma_x^{1-2} \\ \gamma_y^{1-2} \\ \gamma_z^{1-2} \end{bmatrix} \tag{2}$$

and

$$\begin{bmatrix} w_x \\ w_y \\ w_z \end{bmatrix} = \begin{bmatrix} \gamma_x^{1-4} \gamma_y^{1-4} \gamma_z^{1-4} \end{bmatrix} \times \begin{bmatrix} u_x \\ u_y \\ u_z \end{bmatrix} \tag{3}$$

The second direction, the vector $\overline{\gamma}$, is defined by taking the cross product of $\overline{w}$ and $\overline{u}$,

$$\begin{bmatrix} \gamma_x \\ \gamma_y \\ \gamma_z \end{bmatrix} = \begin{bmatrix} w_x w_y w_z \end{bmatrix} \times \begin{bmatrix} u_x \\ u_y \\ u_z \end{bmatrix} \tag{4}$$

The transformation matrix, $\overline{\lambda}$, is created from the direction cosines between the local system and the global system. The nodal coordinates are then multiplied by the transformation matrix.

The pressure load, like the displacements in an isoparametric finite element, is defined anywhere in the element (or on the element face for 3D elements) by

$$q(u,v) = \sum_{i=1}^{n} q_i \Psi_i \tag{5}$$

where:

$q(u,v)$ = the spatial distribution of the pressure load in the local element coordinate system

q_i = the pressure at the nodes

Ψ_i = the element interpolation functions

The equivalent nodal forces are calculated from the exact integral evaluated using the Gauss-Legendre quadrature

$$\bar{q} = \int_{\Omega_R} q(\xi,\eta) d\xi d\eta \cong \sum_{I=1}^{M} \sum_{J=1}^{N} q(\xi_i,\eta_i) \det(J) W_I W_J \tag{6}$$

where:

ξ,η = the element parametric coordinates

$q(\xi,\eta)$ = the pressure distribution in the element's parametric coordinate system

$\det(J)$ = the determinate of the Jacobian

$q(\xi_i,\eta_i)$ = the pressure at the integration points ξ_i,η_i

W_I, W_J = the Gauss-Legendre integration weights

Once calculated, the nodal loads are transformed into the global system using the transpose of transformation matrix.

4. CONTROL DEVICE ANALYSIS

Control devices are those components of an air vehicle that can be directly deflected to affect the trajectory of the vehicle. Examples include elevators, rudders, spoilers, and flaps. All of these are aerodynamic control surfaces. However, "Control Device" encompasses a second set of parameters that have a more general definition: any parameter whose perturbation causes a change in an applied load. Examples from the more general set are the angle-of-attack and the vertical acceleration. Typically these values result from pilot inputs to "control surfaces", but in the simulation process we have access to these "control device" to simulate prescribed quasi-static maneuvers. Both kinds of devices are defined through this interface.

One of the components of an aeroelastic model in FEM analysis is the structural model. In this article , these structural models are presumed to exist (see Figure 1.).

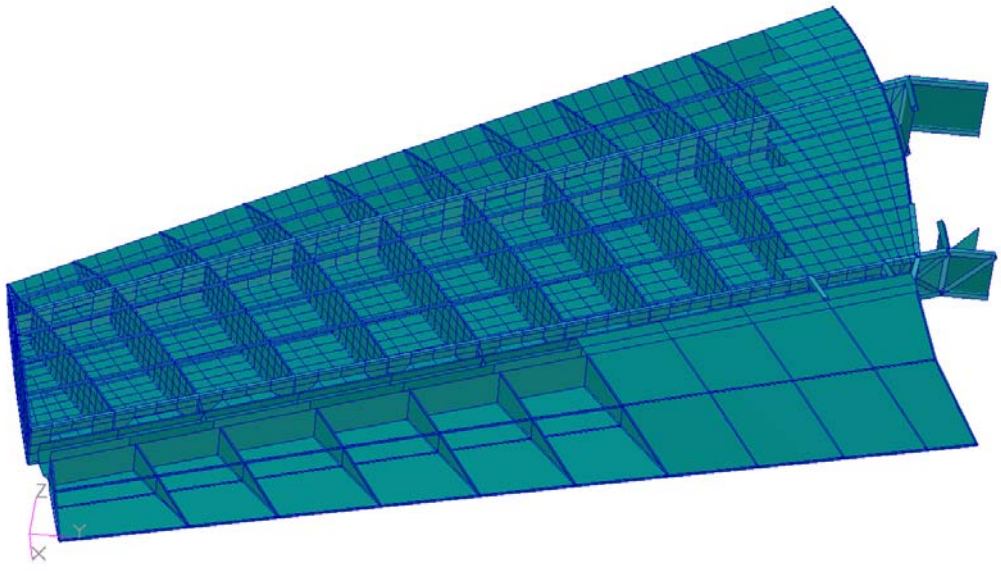

Fig. 1. Horizontal tail stabilizer and elevator assy. – FEM example

5. APPLICATION – HORIZONTAL TAIL EXAMPLE

General data			Elevator data		
bh	span (m)	6.885	**be**	elevator span (m)	2.744
c0h	chord at y=0 (m)	2.706	**c0e**	inner chord (m)	0.931
ceh	chord at tip (m)	1.356	**cee**	outer chord (m)	0.506
Λ0h	l e sweep angle (deg)	31.165	**Λ0e**	l e sweep angle (deg)	20.170
Λ1h	t e sweep angle (deg)	12.000	**Λee**	t e sweep angle (deg)	12.000
Δh	dihedral (deg)	-5.000	**Λeax**	sweep angle at hinge (deg)	20.000
xhax	tail hinge abscissa (m)	1.651	**xeax**	hinge abscissa at c0e (m)	1.954
δhmin	min defl angle (deg)	-15.000	**δemin**	min defl angle (deg)	-25.000
δhmax	max defl angle (deg)	5.000	**δemax**	max defl angle (deg)	25.000
sh	semi-span (m)	3.443	**y0e**	ordinate (y) at c0e (m)	0.500
λh	taper ratio	0.501	**yee**	ordinate (y) at cee (m)	3.244
Sh	h t area (m^2)	13.982	**c0he**	h t chord at y0e	2.510
ARh	aspect ratio	3.390	**cehe**	h t chord at yee	1.433
cmah	mean aero ch (m)	2.106	**Se**	elevator area (total, m^2)	3.942
ycmah	mean aero ch position (m)	1.531			
x25h	abscissa of 0.25 cmah (m)	1.452			
z2	Tip vertical displacement (due to diheral angle)	-0.300012473			
	HT Apex coordinates	x = 15.3490353 y = 0 z = -435.16			

Tab. 1. Horizontal tail geometry (ref. [8])

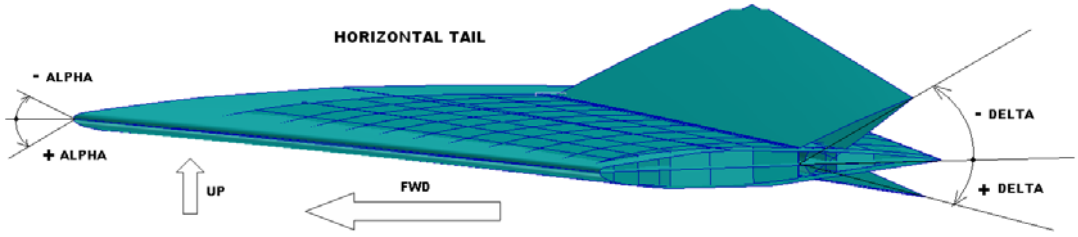

Fig. 2. Angles – Sign conventions

MACH=0.3, H=1000 m						MACH=0.75, H=10000 m					
NAME	ALPHA [deg]	DELTA [deg]	T0 [Kgf]	X0 [m]	Y0 [m]	NAME	ALPHA [deg]	DELTA [deg]	T0 [Kgf]	X0 [m]	Y0 [m]
HT_01	-3.68	-25	-3210.6	1.940	1.789	HT_12	4.70	-25	-3215.3	2.307	1.875
HT_02	-6.78	-20	-3209.2	1.874	1.780	HT_13	1.66	-20	-3213.0	2.162	1.847
HT_03	-9.87	-15	-3207.7	1.808	1.770	HT_14	-1.39	-15	-3210.7	2.017	1.819
HT_04	-12.97	-10	-3206.3	1.741	1.760	HT_15	-4.43	-10	-3208.5	1.872	1.791
HT_05	-16.06	-5	-2772.7	1.479	1.753	HT_16	-7.48	-5	-3206.2	1.726	1.763
HT_06	-19.15	0	-2850.0	1.445	1.741	HT_17	-10.52	0	-3203.9	1.580	1.735
HT_07	-22.25	5	-3202.0	1.542	1.731	HT_18	-13.57	5	-3201.7	1.435	1.707
HT_08	-25.34	10	-3200.6	1.476	1.721	HT_19	-16.61	10	-3199.4	1.289	1.679
HT_09	-28.43	15	-3199.2	1.409	1.711	HT_20	-19.66	15	-3197.1	1.142	1.650
HT_10	-31.53	20	-3196.3	1.276	1.692	HT_21	-22.70	20	-3194.9	.996	1.622
HT_11	-34.62	25	-3197.7	1.343	1.702	HT_22	-25.75	25	-3192.6	.849	1.594

Tab. 2. Horizontal tail 22 limit load cases description (selection)

Table 3 illustrates the Excel® transferred load distribution in the first load case from Table2.

Y [m] / y/b / x/c	3.4 1.00	3.2 0.94	3.0 0.88	2.7 0.79	2.5 0.74	2.3 0.68	2.1 0.62	1.9 0.56	1.7 0.50	1.5 0.44	1.3 0.38	1.1 0.32	0.9 0.26	0.7 0.21	0.5 0.15
1.00	**0**	**0**	**0**	**0**	**0**	**0**	**0**	**0**	**0**	**0**	**0**	**0**	**0**	**0**	**0**
0.99	**12**	**-114**	**-109**	**-102**	**-100**	**-99**	**-97**	**-95**	**-94**	**-92**	**-91**	**-88**	**-83**	**-75**	**-58**
0.96	**20**	**-50**	**-28**	**-2**	**7**	**12**	**16**	**20**	**23**	**27**	**31**	**37**	**53**	**68**	**97**
0.92	**24**	**53**	**84**	**123**	**135**	**143**	**148**	**153**	**156**	**162**	**166**	**172**	**192**	**207**	**236**
0.85	**33**	**154**	**181**	**235**	**251**	**261**	**268**	**273**	**277**	**284**	**288**	**294**	**317**	**331**	**355**
0.78	**44**	**323**	**318**	**388**	**409**	**421**	**429**	**436**	**439**	**448**	**451**	**457**	**483**	**492**	**507**
0.69	**57**	**807**	**533**	**623**	**650**	**664**	**675**	**682**	**685**	**695**	**697**	**701**	**730**	**729**	**728**
0.60	**72**	**696**	**1271**	**1308**	**1316**	**1315**	**1312**	**1306**	**1293**	**1285**	**1260**	**1225**	**1196**	**1083**	**907**
0.50	**89**	**519**	**751**	**786**	**795**	**794**	**791**	**785**	**771**	**764**	**739**	**705**	**689**	**593**	**468**
0.40	**106**	**398**	**565**	**606**	**618**	**618**	**616**	**610**	**595**	**589**	**562**	**528**	**520**	**429**	**323**
0.31	**126**	**318**	**469**	**521**	**537**	**538**	**537**	**531**	**515**	**509**	**480**	**445**	**442**	**351**	**255**
0.22	**150**	**250**	**406**	**474**	**495**	**498**	**498**	**492**	**473**	**468**	**435**	**396**	**400**	**304**	**213**
0.15	**144**	**242**	**425**	**520**	**550**	**557**	**558**	**552**	**530**	**525**	**487**	**441**	**453**	**346**	**256**
0.08	**219**	**251**	**483**	**615**	**657**	**668**	**672**	**666**	**640**	**637**	**590**	**537**	**561**	**440**	**352**
0.04	**554**	**509**	**810**	**991**	**1049**	**1064**	**1069**	**1060**	**1023**	**1018**	**954**	**881**	**921**	**765**	**668**
0.01	**1614**	**1518**	**1865**	**2091**	**2167**	**2174**	**2170**	**2143**	**2066**	**2047**	**1923**	**1786**	**1845**	**1576**	**1426**
0.00	**1614**	**1518**	**1865**	**2091**	**2167**	**2174**	**2170**	**2143**	**2066**	**2047**	**1923**	**1786**	**1845**	**1576**	**1426**

Tab. 3. Pressure load distribution – Load case HT_01

Figure 3 shows the Excel® representation of the pressure distribution from Table 3.

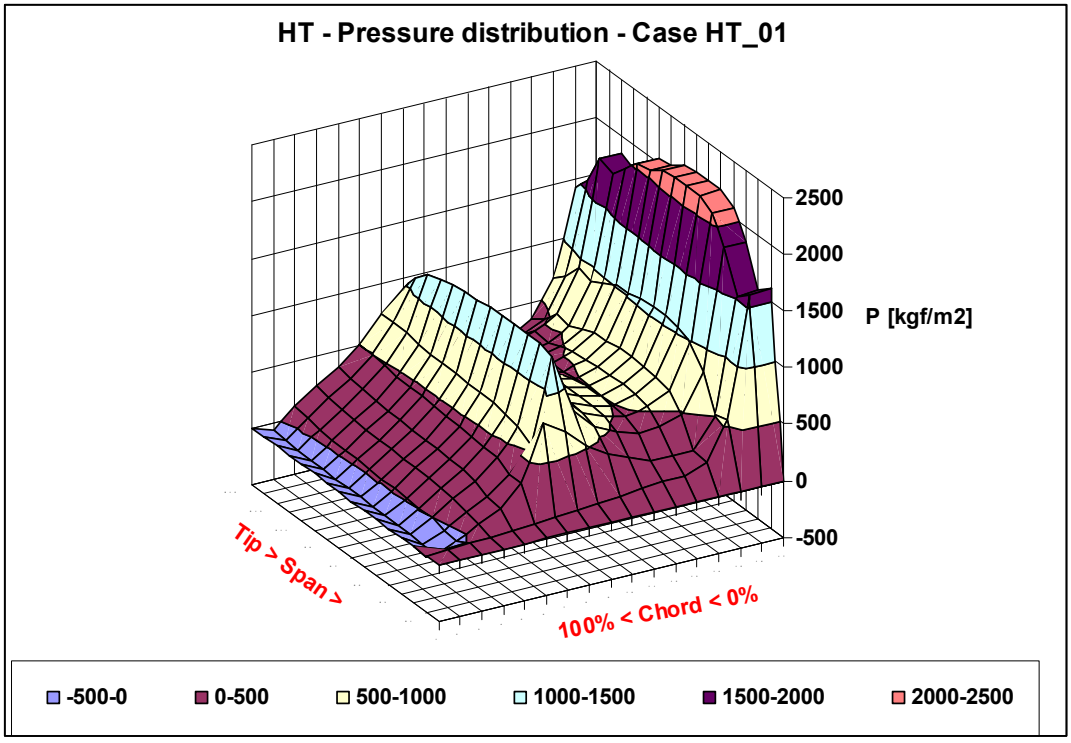

Fig. 3. Pressure load distribution– Load case HT_01

Table 4 illustrates the Excel® transferred load distribution in the last load case from Table2.

Y [m] / y/b / x/c	3.4 1.00	3.2 0.94	3.0 0.88	2.7 0.79	2.5 0.74	2.3 0.68	2.1 0.62	1.9 0.56	1.7 0.50	1.5 0.44	1.3 0.38	1.1 0.32	0.9 0.26	0.7 0.21	0.5 0.15
1.00	0	0	0	0	0	0	0	0	0	0	0	0	0	0	0
0.99	12	-114	-109	-102	-100	-99	-97	-95	-94	-92	-91	-88	-83	-75	-58
0.96	20	-50	-28	-2	7	12	16	20	23	27	31	37	53	68	97
0.92	24	53	84	123	135	143	148	153	156	162	166	172	192	207	236
0.85	33	154	181	235	251	261	268	273	277	284	288	294	317	331	355
0.78	44	323	318	388	409	421	429	436	439	448	451	457	483	492	507
0.69	57	807	533	623	650	664	675	682	685	695	697	701	730	729	728
0.60	72	696	1271	1308	1316	1315	1312	1306	1293	1285	1260	1225	1196	1083	907
0.50	89	519	751	786	795	794	791	785	771	764	739	705	689	593	468
0.40	106	398	565	606	618	618	616	610	595	589	562	528	520	429	323
0.31	126	318	469	521	537	538	537	531	515	509	480	445	442	351	255
0.22	150	250	406	474	495	498	498	492	473	468	435	396	400	304	213
0.15	144	242	425	520	550	557	558	552	530	525	487	441	453	346	256
0.08	219	251	483	615	657	668	672	666	640	637	590	537	561	440	352
0.04	554	509	810	991	1049	1064	1069	1060	1023	1018	954	881	921	765	668
0.01	1614	1518	1865	2091	2167	2174	2170	2143	2066	2047	1923	1786	1845	1576	1426
0.00	1614	1518	1865	2091	2167	2174	2170	2143	2066	2047	1923	1786	1845	1576	1426

Tab. 4. Pressure load distribution – Load case HT_22

Figure 4 shows the Excel® representation of the pressure distribution from Table 4.

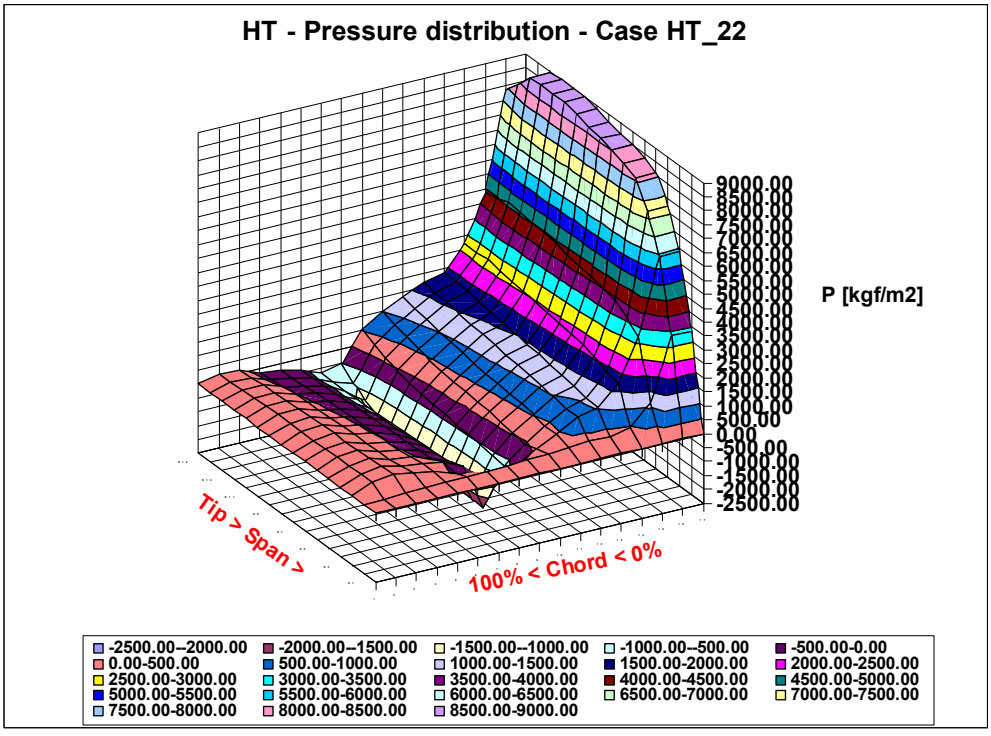

Fig. 4. Pressure load distribution – Load case HT_22

6. LIFTING SURFACE METHODS

A lifting surface is a trapezoidal flat plate that has inboard and outboard edges aligned with the X-axis of the aerodynamic coordinate system as shown in the sketch below.

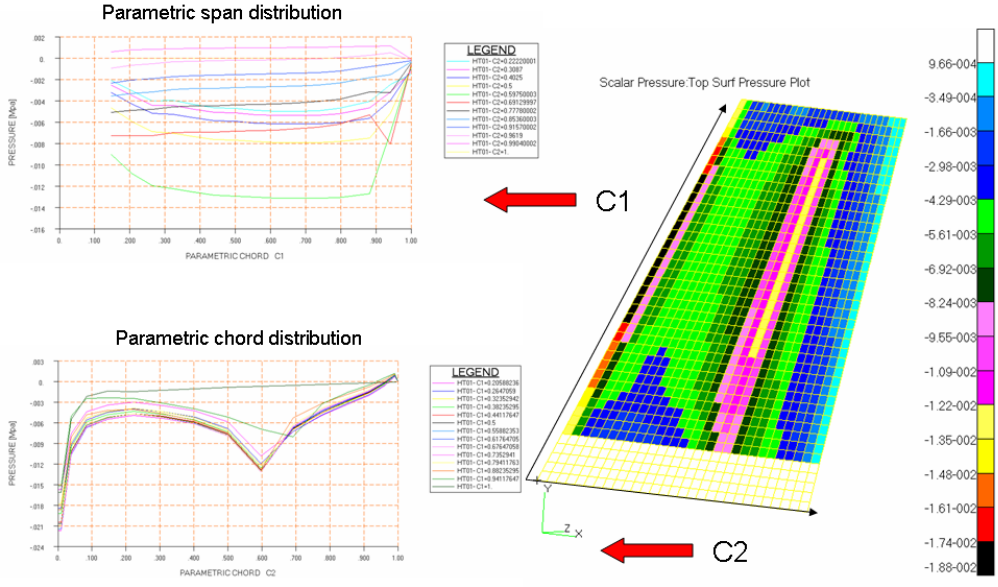

Fig. 5. Lifting Surface

Existing surface is the default method for creating lifting surfaces. This form allows the user to select an existing surface that was either accessed as CAD geometry or created using the geometry application. The surface corners are used to construct the lifting surface, ignoring any surface curvature. Figure 6 shows fields definition, using spatial tabular input, in parametric coordinate system associated to lifting surface defined above.

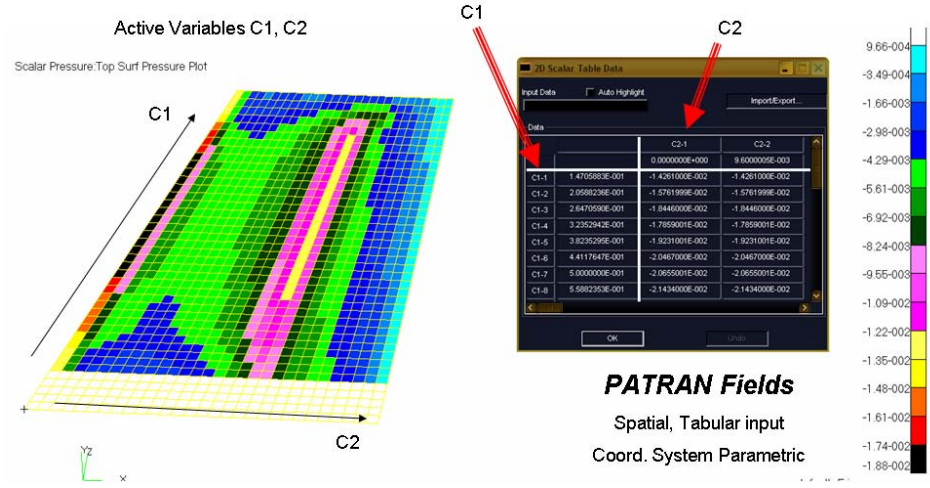

Fig. 6. FEM Fields method

7. CONCLUSIONS

Given the complexity and importance of the loads calculation, it has become a truism with air vehicle design that "the loads are always late". This means that the quantification of the loads is on the critical path in the development of a new or modified vehicle. It also implies that inaccurate initial loads that are corrected or updated after completion of the original structural design can have a serious negative effect on the overall development schedule. In the worst case, if the inaccurate loads are not detected until after the vehicle has entered flight testing, a very costly redesign and retrofitting may have to occur or vehicle placards may be established to limit certain maneuvers, thus reducing the operational performance.

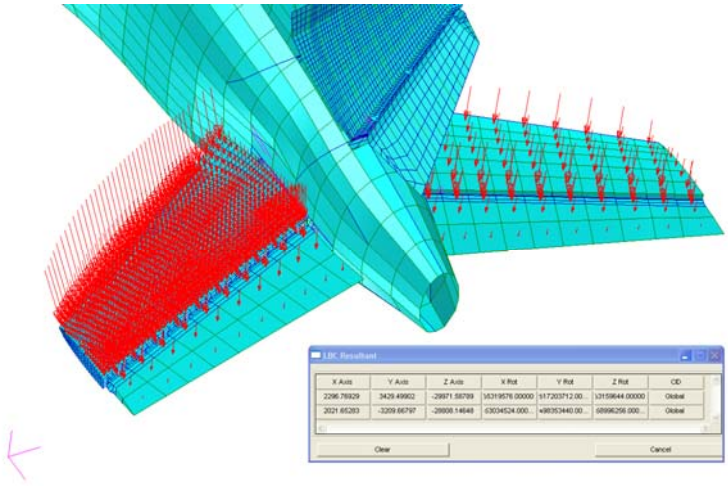

Fig. 7. Pressure load distribution – Load case HT_01 (Limit Load)

REFERENCES

[1.] *** *CS-23 Certification Specifications for Normal, Utility, Aerobatic, and Commuter Category Aero planes*, 14 Nov. 2003.
[2.] *** *MIL HDBK 5J, Metallic Materials and Elements for Aerospace Vehicle Structures*
[3.] E. F. Bruhn., *Analysis and Design of Flight Vehicle Structures, June 1973.*
[4.] M. Niu , Chun Young, *Airframe Stress Analysis and Sizing,* Conmilet Press Ltd, 1998.
[5.] R. J. Roark, W. C. Young*, Formulas for Stress & Strains,* MCGRAW-HILL International, 1989
[6.] A. Petre*, Calculul structurilor de aviatie,* Editura Tehnica Bucuresti, 1984
[7.] G. Vasiliev, V.Giurgiutiu, *Stabilitatea structurilor aeronautice*, Editura Tehnica Bucuresti, 1990
[8.] V. Butoescu, E. Gherega, S. Nebancea*, Aerodynamic polar curves of the tail surfaces; elevator and rudder efficiency*, INCAS Bucuresti, 2010